

Fixation probability in evolutionary dynamics on switching temporal networks

Jnanajyoti Bhaumik¹ Naoki Masuda^{1,2}

¹Department of Mathematics, State University of New York at Buffalo, NY 14260-2900, USA

²Computational and Data-Enabled Science and Engineering Program, State University of New York at Buffalo, Buffalo, NY 14260-5030, USA

Abstract

Population structure has been known to substantially affect evolutionary dynamics. Networks that promote the spreading of fitter mutants are called amplifiers of natural selection, and those that suppress the spreading of fitter mutants are called suppressors. Research in the past two decades has found various families of amplifiers while suppressors still remain somewhat elusive. It has also been discovered that most networks are amplifiers under the birth-death updating combined with uniform initialization, which is a standard condition assumed widely in the literature. In the present study, we extend the birth-death processes to temporal (i.e., time-varying) networks. For the sake of tractability, we restrict ourselves to switching temporal networks, in which the network structure alternates between two static networks at constant time intervals. We show that, in a majority of cases, switching networks are less amplifying than both of the two static networks constituting the switching networks. Furthermore, most small switching networks are suppressors, which contrasts to the case of static networks.

1 Introduction

Evolutionary dynamics models enable us to study how populations change over time under natural selection and neutral random drift among other factors. Over the past two decades, the population structure, particularly those represented by networks (i.e., graphs), has been shown to significantly alter the spread of mutant types [1–5]. Mutants may have a fitness that is different from the fitness of a resident type, which makes the mutants either more or less likely to produce offsprings. The fitness of each type may vary depending on the type of the neighboring individuals' types as in the case of evolutionary games on networks. On the other hand, the simplest assumption on the fitness is to assume that the fitness of each type is constant over time. This latter case, which we refer to as constant selection, has also been studied as biased voter models, modeling stochastic opinion formation in networks (and well-mixed populations) [6–9].

Networks on which real-world dynamical processes approximated by evolutionary dynamics occur may be time-varying. Temporal (i.e., time-varying) networks and dynamical processes on them have been extensively studied [10–16]. Evolutionary game dynamics on time-varying networks are no exception. It has been shown that temporal networks enhance the evolution of cooperation as

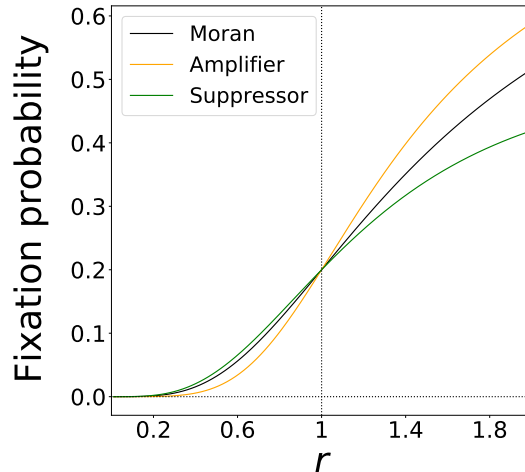


Figure 1: Concept of amplifier and suppressor of natural selection. The fixation probability of a single mutant type for an amplifier is smaller than that for the Moran process when $r < 1$ and larger than that for the Moran process when $r > 1$. Conversely, the fixation probability for a suppressor is larger than that for the Moran process when $r < 1$ and smaller than that for the Moran process when $r > 1$. The Moran process, amplifier, and suppressor have the same fixation probability at $r = 1$, which is equal to $1/N$. In the figure, the fixation probabilities for the Moran process are given by Eq. (9) with $N = 5$, and those for the amplifier and suppressor are hypothetical ones for expository purposes.

compared to static networks [17–20]. It has also been known for a longer time that coevolutionary dynamics of a social dilemma game and network structure, in which the dynamics of the network structure depend on the state of the nodes (e.g., cooperator or defector), enhance overall cooperation if players tend to avoid creating or maintaining edges connecting to defectors [5, 21–23].

In this study, we investigate constant-selection evolutionary dynamics on temporal networks to clarify how the time dependence of the network structure impacts evolutionary processes. In particular, a key question in studies of constant-selection evolutionary dynamics on networks is the fixation probability, defined as the probability that a single mutant type introduced to a node in the network eventually fixates, i.e., occupies all the nodes of the network. The fixation probability depends on the fitness of the mutant type relative to the fitness of the resident type, denoted by r . A network is called an amplifier of natural selection if it has a higher fixation probability than the complete graph, which corresponds to the Moran process, when $r > 1$ and a lower fixation probability when $r < 1$; conversely, a network is called a suppressor if the fixation probability is smaller than for the Moran process on $r > 1$ and larger for $r < 1$ [1, 24]. In Fig. 1, we show hypothetical examples of the fixation probability as a function of r for three networks: the complete graph (i.e., Moran process), an amplifier, and a suppressor. Under the so-called birth-death updating rule and uniform initialization, most static networks are amplifiers [25, 26]. In fact, there is only one suppressing static network with six nodes among the 112 connected six-node networks [27].

Furthermore, various families of amplifiers have been found [28–32], whereas suppressors still

remain elusive [27, 33]. On these grounds, we ask the following two main questions in the present study. First, as in the case of static networks, is a vast majority of temporal networks amplifier of natural selection under the same condition (i.e., birth-death updating rule and uniform initialization)? Second, if we combine amplifying static networks, G_1 and G_2 , into a temporal network, can the obtained temporal network be a suppressor or a less amplifying temporal network than both G_1 and G_2 ?

2 Model

Let G be a static weighted network with N nodes. We assume undirected networks for simplicity although extending the following evolutionary dynamics to the case of directed networks is straightforward. We assume that each node takes either the resident or mutant type at any discrete time. The resident and mutant have fitness 1 and r , respectively. The fitness represents the propensity with which each type is selected for reproduction in each time step. The mutant type initially occupies just one node, which is selected uniformly at random among the N nodes. The other $N - 1$ nodes are occupied by the resident type. We then run the birth-death process, which is a generalization of the Moran process to networks [1, 3–5, 34, 35]. Specifically, in every discrete time step, we select a node v to reproduce with the probability proportional to its fitness value. Next, we select a neighbor of v , denoted by v' , with the probability proportional to the weight of the undirected edge (v, v') . Then, the type at v (i.e., either resident or mutant) replaces that at v' . We repeat this process until the entire population is of a single type, either resident or mutant, which we call the fixation.

In this study, we extend this birth-death process to temporal networks in which two static networks G_1 and G_2 , both having N nodes, alternate with constant intervals τ . We call this temporal network model the switching network and denote it by (G_1, G_2, τ) . Switching networks have been used for studying various dynamics on temporal networks including synchronization [35–41], random walk [42–44], epidemic processing [45–48], network control [49], and reaction-diffusion systems [50]. Specifically, we first run the birth-death process on G_1 for τ time steps. Then, we switch to G_2 and run the same birth-death process on G_2 for τ time steps. Then, we switch back to G_1 . We keep flipping between G_1 and G_2 every τ time steps until the fixation of either type occurs.

3 Computation and theoretical properties of the fixation probability in switching networks

In this section, we describe the methods for calculating the fixation probability of a single mutant, i.e., the probability that the mutant type of fitness r fixates when there is initially just one node of the mutant type that is selected uniformly at random. We extend the methods for static networks [51] to our model. We also state some mathematical properties of the fixation probability in switching networks.

3.1 Fixation probability in static networks

We first explain the known procedure for calculating the fixation probability of the mutant type, which we simply refer to as the fixation probability in the following text, in any static weighted

network using Markov chains [1, 51]. We describe the state of the evolutionary dynamics by an N -dimensional binary vector $\mathbf{s} = (s_1, \dots, s_N)$, where $s_i \in \{0, 1\}, \forall i \in \{1, \dots, N\}$. For each i , let $s_i = 0$ or $s_i = 1$ indicate that node i is occupied by a resident or a mutant, respectively. Let S be the set of all states. Note that S has cardinality 2^N , that is, there are 2^N states and that there are $\binom{N}{m}$ states with m mutants. We label the states by a bijective map, denoted by f , from S to $\{1, \dots, 2^N\}$. The transition probability matrix of the Markov chain, denoted by $T = (T_{ij})$, is a $2^N \times 2^N$ matrix. Its entry $T_{f(\mathbf{s}), f(\mathbf{s}')}$ represents the probability that the state changes from \mathbf{s} to \mathbf{s}' in one time step. It should be noted that $T_{f(\mathbf{s}), f(\mathbf{s}')}$ can be non-zero if and only if vectors \mathbf{s} and \mathbf{s}' differ in at most one entry. Therefore, each row of T has at most $N + 1$ non-zero entries.

Let \mathbf{s} be a state with m mutants, $s_i = 1$ for $i \in \{g(1), \dots, g(m)\}$, and $s_i = 0$ for $i \in \{g(m+1), \dots, g(N)\}$, where g is a permutation on $\{1, \dots, N\}$. Let \mathbf{s}' be the state with $m + 1$ mutants in which $s'_i = 1$ for $i \in \{g(1), \dots, g(m), g(m+1)\}$ and $s'_i = 0$ for $i \in \{g(m+2), \dots, g(N)\}$. Note that \mathbf{s} and \mathbf{s}' differ only at the $g(m+1)$ th node, where \mathbf{s} has a resident and \mathbf{s}' has a mutant. We obtain

$$T_{f(\mathbf{s}), f(\mathbf{s}')} = \frac{r}{rm + N - m} \sum_{m'=1}^m \frac{A_{g(m'), g(m+1)}}{w(g(m'))}, \quad (1)$$

where A denotes the weighted adjacency matrix of the network, i.e., A_{ij} is the weight of edge (i, j) , and $w(i) \equiv \sum_{j=1}^N A_{ij}$ represents the weighted degree of the i th node, also called the strength of the node. Next, consider a state \mathbf{s}'' with $m - 1$ mutants such that $s''_i = 1$ for $i \in \{g(1), \dots, g(\tilde{m} - 1), g(\tilde{m} + 1), \dots, g(m)\}$ and $s''_i = 0$ for $i \in \{g(\tilde{m}), g(m+1), g(m+2), \dots, g(N)\}$. We obtain

$$T_{f(\mathbf{s}), f(\mathbf{s}'')} = \frac{1}{rm + N - m} \sum_{m'=m+1}^N \frac{A_{g(m'), g(\tilde{m})}}{w(g(m'))}. \quad (2)$$

The probability that the state does not change after one time step is given by

$$T_{f(\mathbf{s}), f(\mathbf{s})} = 1 - \frac{r}{rm + N - m} \sum_{\ell=m+1}^N \sum_{m'=1}^m \frac{A_{g(m'), g(\ell)}}{w(g(m'))} - \frac{1}{rm + N - m} \sum_{\tilde{m}=1}^m \sum_{m'=m+1}^N \frac{A_{g(m'), g(\tilde{m})}}{w(g(m'))}. \quad (3)$$

Let $x_{f(\mathbf{s})}$ denote the probability that the mutant fixates when the evolutionary dynamics start from state \mathbf{s} . Because

$$x_{f(\mathbf{s})} = \sum_{\mathbf{s}' \in S} T_{f(\mathbf{s}), f(\mathbf{s}')} x_{f(\mathbf{s}')}, \quad (4)$$

we obtain $T\mathbf{x} = \mathbf{x}$, where $\mathbf{x} = (x_1, \dots, x_{2^N})^\top$, and \top represents the transposition. Because $x_{f((0, \dots, 0))} = 0$ and $x_{f((1, \dots, 1))} = 1$, we need to solve the set of $2^N - 2$ linear equations to obtain the fixation probabilities starting from an arbitrary initial state.

3.2 Fixation probability in switching networks

We now consider the same birth-death process on switching network (G_1, G_2, τ) . To calculate the fixation probability in (G_1, G_2, τ) , we denote by $T^{(1)}$ and $T^{(2)}$ the transition probability matrices for the birth-death process on static network G_1 and G_2 , respectively. Let $x_i(t)$ be the fixation probability when the evolutionary dynamics start from the i th state (with $i \in \{1, \dots, 2^N\}$) at time

t. We obtain

$$\mathbf{x}(t) = \begin{cases} T^{(1)}\mathbf{x}(t+1) & \text{if } 2n\tau \leq t < (2n+1)\tau, \\ T^{(2)}\mathbf{x}(t+1) & \text{if } (2n+1)\tau \leq t < (2n+2)\tau, \end{cases} \quad (5)$$

where $\mathbf{x}(t) = (x_1(t), \dots, x_{2N}(t))^\top$ and $n \in \{0, 1, \dots\}$. We recursively use Eq. (5) to obtain

$$\begin{aligned} \mathbf{x}(0) &= T^{(1)}\mathbf{x}(1) = \dots = \left(T^{(1)}\right)^\tau \mathbf{x}(\tau) = \left(T^{(1)}\right)^\tau \left(T^{(2)}\right) \mathbf{x}(\tau+1) = \dots \\ &= \left(T^{(1)}\right)^\tau \left(T^{(2)}\right)^\tau \mathbf{x}(2\tau). \end{aligned} \quad (6)$$

Because of the periodicity of the switching network, we obtain $\mathbf{x}(0) = \mathbf{x}(2\tau)$. Therefore, the fixation probability is given as the solution of

$$\mathbf{x}^* = \left(T^{(1)}\right)^\tau \left(T^{(2)}\right)^\tau \mathbf{x}^*. \quad (7)$$

Let $\tilde{S}^{(1)}$ be the set of the N states with just one mutant. Then, the fixation probability when there is initially a single mutant located on a node that is selected uniformly at random is given by

$$\rho \equiv \frac{1}{N} \sum_{s \in \tilde{S}^{(1)}} x_{f(s)}^*. \quad (8)$$

Note that ρ is a function of r and depends on the network structure. Because $\left(T^{(1)}\right)^\tau \left(T^{(2)}\right)^\tau$ is a stochastic matrix with two absorbing states, it has a unique solution [52, 53].

The birth-death process on switching networks has the following property.

Theorem 1. (*Neutral drift*) *If $r = 1$, then $\rho = \frac{1}{N}$ for arbitrary G_1, G_2 , and $\tau \in \mathbb{N}$.*

Proof. We imitate the proof given in [54]. Assume a switching network (G_1, G_2, τ) on N nodes and that each node is initially occupied by a mutant of distinct type, i.e., node i is occupied by a mutant of type A_i . We also assume that each mutant has fitness 1. We denote the probability that mutant A_i fixates by q_i . Note that $\sum_{i=1}^N q_i = 1$. Now we reconsider our original evolutionary dynamics with $r = 1$, in which there are only equally strong two types, i.e., resident type and mutant type, with the initial condition in which the mutant type occupies the i th node and the resident type occupies all the other $N - 1$ nodes. Then, the fixation probability of the mutant is equal to q_i because this model is equivalent to the previous model if we identify A_i with the mutant type and the other $N - 1$ types with the resident type. Therefore, the fixation probability for the original model with $r = 1$ and the uniform initialization is given by $\sum_{i=1}^N q_i/N = 1/N$. \square

Remark. The theorem holds true even if we switch among more than two static networks or if the switching intervals, τ , deterministically change from one switching interval to another. The proof remains unchanged.

3.3 Identifying amplifiers and suppressors

We operationally define amplifiers and suppressors as follows; similar definitions were used in the literature [1, 55]. For a given switching or static network, we computed the fixation probability for

several values of r . We say that the network is amplifier if the fixation probability is larger than for that for the complete graph with the same number of nodes, or equivalently, the Moran process, at six values of $r > 1$, i.e., $r \in \{1.1, 1.2, 1.3, 1.4, 1.6, 1.8\}$ and a smaller than that for the Moran process at three values of $r < 1$, i.e., $r \in \{0.7, 0.8, 0.9\}$. Note that the fixation probability for the Moran process with N individuals is given by (see e.g. [2])

$$\rho = \frac{1 - \frac{1}{r}}{1 - \frac{1}{r^N}}. \quad (9)$$

Similarly, we say that a network is suppressor if the fixation probability is smaller than for the Moran process at the same six values of r larger than 1 and larger than for the Moran process at the three values of r smaller than 1. It is known that some static networks are neither amplifier nor suppressor [33].

3.4 Isothermal theorem

A network is called isothermal if its fixation probability is the same as that for the Moran process, i.e., if Eq. (9) holds true [1]. A static undirected network, which may be weighted, is isothermal if and only if all the nodes have the same (weighted) degree [1, 56, 57]. One can easily construct isothermal switching networks as follows.

Theorem 2. *If G_1 and G_2 are isothermal networks, then the switching network (G_1, G_2, τ) is an isothermal network.*

Proof. The proof is exactly the same as in the static network case as shown in [1, 2]. We denote by $p_{m,m-1}$ the probability that the state of the network moves from a state with m mutants to a state with $m - 1$ mutants in one time step. Similarly, we denote by $p_{m,m+1}$ the probability that the state moves from one with m mutants to one with $m + 1$ mutants in one time step. We observe that $p_{m,m-1}/p_{m,m+1} = 1/r$ at every time step t because the static network at any t , which is either G_1 or G_2 , is isothermal. Therefore, the fixation probability for (G_1, G_2, τ) is given by Eq. (9). \square

4 Fixation probability in various switching networks

In this section, we analyze the fixation probability in three types of switching networks, i.e., networks with six nodes, larger switching networks in which G_1 and G_2 have symmetry (i.e., complete graph, star graph, and bipartite networks), and empirical networks.

4.1 Six-node networks

We first analyzed the fixation probability in switching networks that are composed of two undirected and unweighted connected networks with 6 nodes. There are 112 non-isomorphic undirected connected networks on 6 nodes. We switched between any ordered pair of different networks, giving us a total of $112 \times 111 = 12432$ switching networks. It should be noted that swapping the order of G_1 and G_2 generally yields different fixation probabilities. We randomly permuted the node labels in G_2 . We did not consider all possible labeling of nodes because there would be at most $112 \cdot 111 \cdot 6! = 8951040$ switching networks on 6 nodes if we allow shuffling of node labeling, although the symmetry reduces this number.

In Fig. 2(a), we show two arbitrarily chosen static networks on six nodes, G_1 and G_2 , which are amplifiers as static networks. In Fig. 2(b), we plot the fixation probability as a function of the fitness of the mutant, r , for the switching network $(G_1, G_2, \tau = 1)$, the static networks G_1 and G_2 , the aggregate weighted static network generated from G_1 and G_2 , and the Moran process (i.e., complete graph on six nodes). The aggregated weighted static network is the superposition of G_1 and G_2 such that the weight of the edge is either 1 or 2. It is equivalent to the average of G_1 and G_2 over time. All these static and switching networks yield $\rho = 1/N = 1/6$ at $r = 1$, as expected (see Theorem 1). In addition, there exist differences in ρ between the different networks and the Moran process although the difference is small. In fact, G_1 and G_2 are amplifiers, with their fixation probability being larger than that for the Moran process when $r > 1$ and vice versa when $r < 1$, confirming the known result [25, 27]. Figure 2(b) also indicates that the aggregate network is an amplifier. However, the switching network is suppressor.

We reconfirm these results in Fig. 2(c), in which we show the difference in the fixation probability between a given static or switching network and the Moran process. If the difference is negative for $r < 1$ and positive for $r > 1$, then the network is an amplifier. If the difference is positive for $r < 1$ and negative for $r > 1$, then the network is a suppressor. Figure 2(c) shows that G_1 is a stronger amplifier than G_2 , which is a stronger amplifier than the aggregate network. In contrast, the switching network $(G_1, G_2, 1)$ is a suppressor while $(G_1, G_2, 10)$ and $(G_1, G_2, 50)$ are amplifiers. The result for $(G_1, G_2, 50)$ is close to that for static network G_1 , which is because the evolutionary dynamics on (G_1, G_2, τ) is equivalent to that on G_1 in the limit $\tau \rightarrow \infty$. We conclude that switching networks composed of two amplifiers can be a suppressor, in particular when τ is small. We emphasize that this counterintuitive result is not due to the property of the aggregate network because the aggregate network, which is the time average of G_1 and G_2 , is also an amplifier.

To investigate the generality of this finding to other six-node networks, we calculated the fixation probability for the switching networks derived from all possible pairs of six-node networks. Table 1 shows the number of switching networks on six nodes that are amplifiers, that of suppressors, and that of networks that are neither amplifier or suppressor, for four values of τ . The table indicates that a majority of the six-node switching networks investigated are suppressors when $\tau = 1$ and $\tau = 3$. This result is in stark contrast to the fact that there is only 1 suppressor among 112 six-node static unweighted networks under the birth-death process [25, 27]. Out of the 111 static networks that are not suppressor, 100 networks are amplifiers, five are isothermal, and the other six networks are neither amplifier, suppressor, nor isothermal [33, 58]. Most switching networks are amplifiers when $\tau = 50$, which is presumably because most static networks are amplifiers and the birth-death process on (G_1, G_2, τ) converges to that on G_1 in the limit $\tau \rightarrow \infty$, as we discussed above.

4.2 Larger symmetric switching networks

In this section, we assume symmetry in G_1 and G_2 to calculate the fixation probability for larger switching networks. Specifically, we set G_1 to be the star graph and G_2 to be either the complete graph or complete bipartite graph.

4.2.1 Combination of the star graph and the complete graph

Consider switching networks in which G_1 is the star graph and G_2 is the complete graph. For this switching network, we can reduce the dimension of the transition probability matrix from $2^N \times 2^N$ to $2N \times 2N$ by exploiting the symmetry in G_1 and G_2 . Therefore, one can reduce the number of equations from $2^N - 2$ to $2N - 2$. Specifically, one can uniquely describe the state of the network

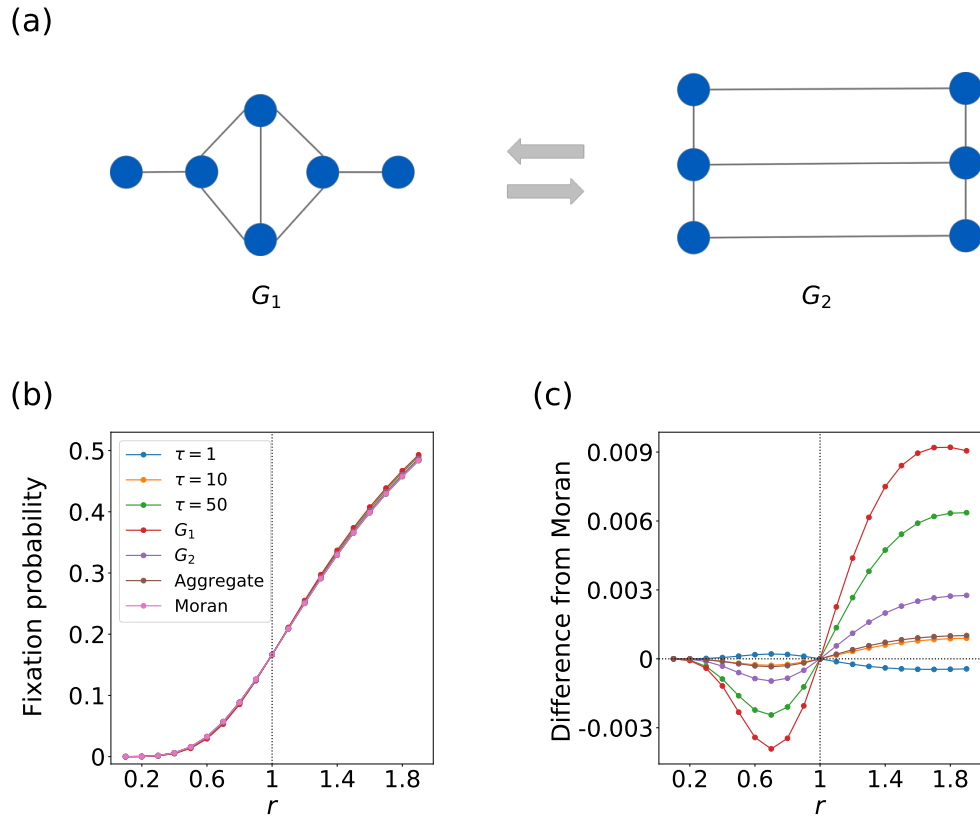


Figure 2: A suppressing switching network composed of two amplifying static networks on six nodes. (a) A switching network composed of six nodes. Both G_1 and G_2 are amplifiers. (b) Fixation probability in the static and switching networks as a function of r . Moran refers to the Moran process. Note that G_1 , G_2 , the aggregate network, and the Moran process represent static networks. (c) Difference between the fixation probability for the given network and that for the Moran process.

Table 1: Number of amplifiers and suppressors among $112 \cdot 111 = 12432$ switching networks on six nodes.

τ	Amplifier	Suppressor	Neither
1	3636	8177	619
3	5190	6347	895
10	11102	629	701
50	12038	262	132

by (i, j) , where $i \in \{0, 1\}$ and $j \in \{0, \dots, N - 1\}$. We set $i = 0$ and $i = 1$ when the hub node of G_1 is occupied by a resident or mutant, respectively. We set $j \in \{0, 1, \dots, N - 1\}$ to the number of mutants in the other $N - 1$ nodes, which we refer to as the leaves. Tuple (i, j) is a valid expression of the state of the network because the $N - 1$ leaves are structurally equivalent to each other in both G_1 and G_2 . Tuples $(0, 0)$ and $(1, N - 1)$ correspond to the fixation of the resident and mutant type, respectively.

The transition probability from state (i, j) to state (i', j') in a single time step of the birth-death process is nonzero if and only if $(i', j') = (i, j + 1)$ and $i = 1$, $(i', j') = (i, j - 1)$ and $i = 0$, $(i', j') = (1 - i, j)$, or $(i', j') = (i, j)$. Let $T^{(1)}$ denote the transition probability matrix for the star graph. We obtain

$$T_{(i,j) \rightarrow (i',j')}^{(1)} = \begin{cases} \frac{rj}{C_1} & \text{if } i = 0 \text{ and } i' = 1, \\ \frac{N-1-j}{C_2} & \text{if } i = 1 \text{ and } i' = 0, \\ \frac{1}{C_1} \cdot \frac{j}{N-1} & \text{if } i' = i = 0 \text{ and } j' = j - 1, \\ \frac{r}{C_2} \cdot \frac{N-1-j}{N-1} & \text{if } i' = i = 1 \text{ and } j' = j + 1, \\ 1 - \sum_{\substack{(i'',j'') \neq \\ (i,j)}} T_{(i,j) \rightarrow (i'',j'')}^{(1)} & \text{if } (i', j') = (i, j), \\ 0 & \text{otherwise,} \end{cases} \quad (10)$$

where $C_1 = rj + N - j$ and $C_2 = r(j + 1) + N - (j + 1)$ [1]. The first line of Eq. (10) represents the probability that the type of the hub changes from the resident to mutant. For this event to occur, one of the j leaf nodes occupied by the mutant must be chosen as parent, which occurs with probability $rj / (rj + N - j)$. Because every leaf node is only adjacent to the hub node, the hub node is always selected for death if a leaf node is selected as parent. Therefore, the probability of i changing from 0 to 1 is equal to $rj / (rj + N - j)$, which is shown in the first line of Eq. (10). As another example, consider state $(1, j)$, in which the hub has a mutant, j leaf nodes have mutants, and the other $N - 1 - j$ leaf nodes have residents. For the state to change from $(1, j)$ to $(1, j + 1)$, the hub node must be selected as parent with probability $r / [r(j + 1) + N - (j + 1)]$, and a leaf node of the resident type must be selected for death, which occurs with probability $(N - 1 - j) / (N - 1)$. The fourth line of Eq. (10) is equal to the product of these two probabilities. One can similarly derive the other lines of Eq. (10).

The transition probability matrix for G_2 , which is the complete graph, is given by

$$T_{(i,j) \rightarrow (i',j')}^{(2)} = \begin{cases} \frac{rj}{C_1} \cdot \frac{1}{N-1} & \text{if } i = 0 \text{ and } i' = 1, \\ \frac{N-1-j}{C_2} \cdot \frac{1}{N-1} & \text{if } i = 1 \text{ and } i' = 0, \\ \frac{N-j}{C_1} \cdot \frac{j}{N-1} & \text{if } i' = i = 0 \text{ and } j' = j - 1, \\ \frac{rj}{C_1} \cdot \frac{N-1-j}{N-1} & \text{if } i' = i = 0 \text{ and } j' = j + 1, \\ \frac{N-1-j}{C_2} \cdot \frac{j}{N-1} & \text{if } i' = i = 1 \text{ and } j' = j - 1, \\ \frac{r(j+1)}{C_2} \cdot \frac{N-1-j}{N-1} & \text{if } i' = i = 1 \text{ and } j' = j + 1, \\ 1 - \sum_{\substack{(i'',j'') \neq \\ (i,j)}} T_{(i,j) \rightarrow (i'',j'')}^{(1)} & \text{if } (i', j') = (i, j), \\ 0 & \text{otherwise.} \end{cases} \quad (11)$$

For example, for the transition from state $(0, j)$ to $(1, j)$ to occur, one of the j mutant leaf nodes must be first selected as parent, which occurs with probability $rj / (rj + N - j)$. Then, the hub node must be selected for death, which occurs with probability $1 / (N - 1)$. The first line of Eq. (11) is equal to the product of these two probabilities. As another example, for the state to change from $(1, j)$ to $(1, j + 1)$, one of the mutant nodes, which may be the hub or a leaf, must be first selected as parent, which occurs with probability $r(j + 1) / [r(j + 1) + N - (j + 1)]$. Then, a leaf node of the resident type must be selected for death, which occurs with probability $(N - 1 - j) / (N - 1)$. The right-hand side on the sixth line of Eq. (11) is equal to the product of these two probabilities. One can similarly derive the other lines of Eq. (11). It should be noted that single-step moves from $(1, j)$ to $(1, j - 1)$ and those from $(0, j)$ to $(0, j + 1)$ are possible in G_2 , whereas they do not occur in G_1 .

In Fig. 3(a), we plot the fixation probability as a function of r for switching network (G_1, G_2, τ) in which G_1 is the star graph and G_2 is the complete graph on four nodes. In this figure, we compare (G_1, G_2, τ) with $\tau = 1, 10$, and 50 , the static star graph, the aggregate network, and the Moran process. Figure 3(a) indicates that $(G_1, G_2, 10)$ and $(G_1, G_2, 50)$ are amplifiers and that $(G_1, G_2, 1)$ is a suppressor. We plot the difference in the fixation probability between the switching networks and the Moran process in Fig. 3(b). When $\tau = 1$, the difference is positive for $r < 1$ and negative for $r > 1$, which verifies that $(G_1, G_2, 1)$ is a suppressor. This result is surprising because G_1 is an amplifier and G_2 is equivalent to the Moran process and therefore not a suppressor. In contrast, when $\tau = 10$ and $\tau = 50$, the difference from the Moran process is negative for $r < 1$ and positive for $r > 1$, which verifies that $(G_1, G_2, 10)$ and $(G_1, G_2, 50)$ are amplifiers. The result for $\tau = 50$ is close to that for the star graph. This is presumably because the first $\tau = 50$ steps with G_1 are sufficient to induce fixation with a high probability given the small network size (i.e., $N = 4$).

Figures 3(a) and 3(b) also indicate that the aggregate network is a weak suppressor. However, the aggregate network is a considerably weaker suppressor than $(G_1, G_2, 1)$. Therefore, we conclude that the suppressing effect of the switching network mainly originates from the time-varying nature of the network rather than the structure of the weighted aggregate network.

We show in Figs. 3(c) and 3(d) the fixation probability and its difference from the case of the Moran process, respectively, as a function of r for $N = 50$. We observe that the switching network is an amplifier for all the values of τ that we considered, i.e., $\tau = 1, 10$, and 50 . In contrast, the aggregate network is a suppressor albeit an extremely weak one. The amplifying effect of the switching network is stronger for a larger value of τ . Unlike in the case of four nodes (see Figs. 3(a)

and 3(b)), the switching networks with 50 nodes are far less amplifying than the star graph even with $\tau = 50$. This phenomenon is expected because fixation in a static network with 50 nodes usually needs much more than 50 steps.

These results for the switching networks with $N = 4$ and $N = 50$ nodes remain similar for (G_2, G_1, τ) , i.e., when we swap the order of G_1 and G_2 (see Figs. A1(a) and A1(b)).

The present switching network is a suppressor when $N = 4$ and $\tau = 1$ and an amplifier when $N = 50$ or $\tau \in \{10, 50\}$. To examine the generality of these results with respect to the number of nodes, N , we show in Figs. 3(e) and 3(f) the fixation probability relative to that for the Moran process at $\tau = 1$ and $\tau = 50$, respectively, as a function of N . In both figures, we show the fixation probabilities at $r = 0.9$ and $r = 1.1$. Figure 3(e) indicates that the switching network is a suppressor for $N \leq 4$ and an amplifier for $N \geq 5$ when $\tau = 1$. We have confirmed that this switching network with $N = 3$ nodes is a suppressor by calculating the fixation probability across a range of r values in (see Fig. A2(a)). Figure 3(f) indicates that $(G_1, G_2, 50)$ is an amplifier for any N .

4.2.2 Combination of the star graph and the complete bipartite graph

In this section, we analyze the switching network in which G_1 is the star graph and G_2 is the complete bipartite graph K_{N_1, N_2} . By definition, K_{N_1, N_2} has two disjoint subsets of nodes V_1 and V_2 , and V_1 and V_2 contain N_1 and N_2 nodes, respectively. Every node in V_1 is adjacent to every node in V_2 by an edge. Therefore, every node in V_2 is adjacent to every node in V_1 . Without loss of generality, we assume that the hub node in G_1 is one of the N_1 nodes in V_1 .

Because of the symmetry, we do not need to distinguish among the $N_1 - 1$ nodes that are leaf nodes in G_1 and belong to V_1 in G_2 , or among the N_2 nodes that belong to V_2 in G_2 . Therefore, one can specify the state of this switching network by a tuple (i, j, k) , where $i \in \{0, 1\}$ represents whether the hub is occupied by a resident, corresponding to $i = 0$, or mutant, corresponding to $i = 1$; variable $j \in \{0, \dots, N_1 - 1\}$ represents the number of mutants among the $N_1 - 1$ nodes that are leaves in G_1 and belong to V_1 in G_2 ; variable $k \in \{0, \dots, N_2\}$ represents the number of mutants among the N_2 nodes in V_2 . Tuples $(0, 0, 0)$ and $(1, N_1 - 1, N_2)$ correspond to the fixation of the resident and mutant type, respectively. Using this representation of the states, we reduce the $2^N \times 2^N$ transition probability matrix to a $2N_1(N_2 + 1) \times 2N_1(N_2 + 1)$ transition probability matrix.

The transition probability matrix for the star graph is given by

$$T_{(i,j,k) \rightarrow (i',j',k')}^{(1)} = \begin{cases} \frac{r(j+k)}{C_3} & \text{if } i = 0 \text{ and } i' = 1, \\ \frac{N-1-j-k}{C_4} & \text{if } i = 1 \text{ and } i' = 0, \\ \frac{1}{C_3} \cdot \frac{j}{N-1} & \text{if } i = 0 \text{ and } j' = j - 1, \\ \frac{1}{C_3} \cdot \frac{k}{N-1} & \text{if } i = 0 \text{ and } k' = k - 1, \\ \frac{r}{C_4} \cdot \frac{N_1-1-j}{N-1} & \text{if } i = 1 \text{ and } j' = j + 1, \\ \frac{r}{C_4} \cdot \frac{N_2-j}{N-1} & \text{if } i = 1 \text{ and } k' = k + 1, \\ 1 - \sum_{\substack{(i'',j'',k'') \neq \\ (i,j,k)}} T_{(i,j,k) \rightarrow (i'',j'',k'')}^{(1)} & \text{if } (i', j', k') = (i, j, k), \\ 0 & \text{otherwise,} \end{cases} \quad (12)$$

where $C_3 = r(j+k) + (N-j-k)$ and $C_4 = r(j+k+1) + (N-j-k-1)$. The first line of

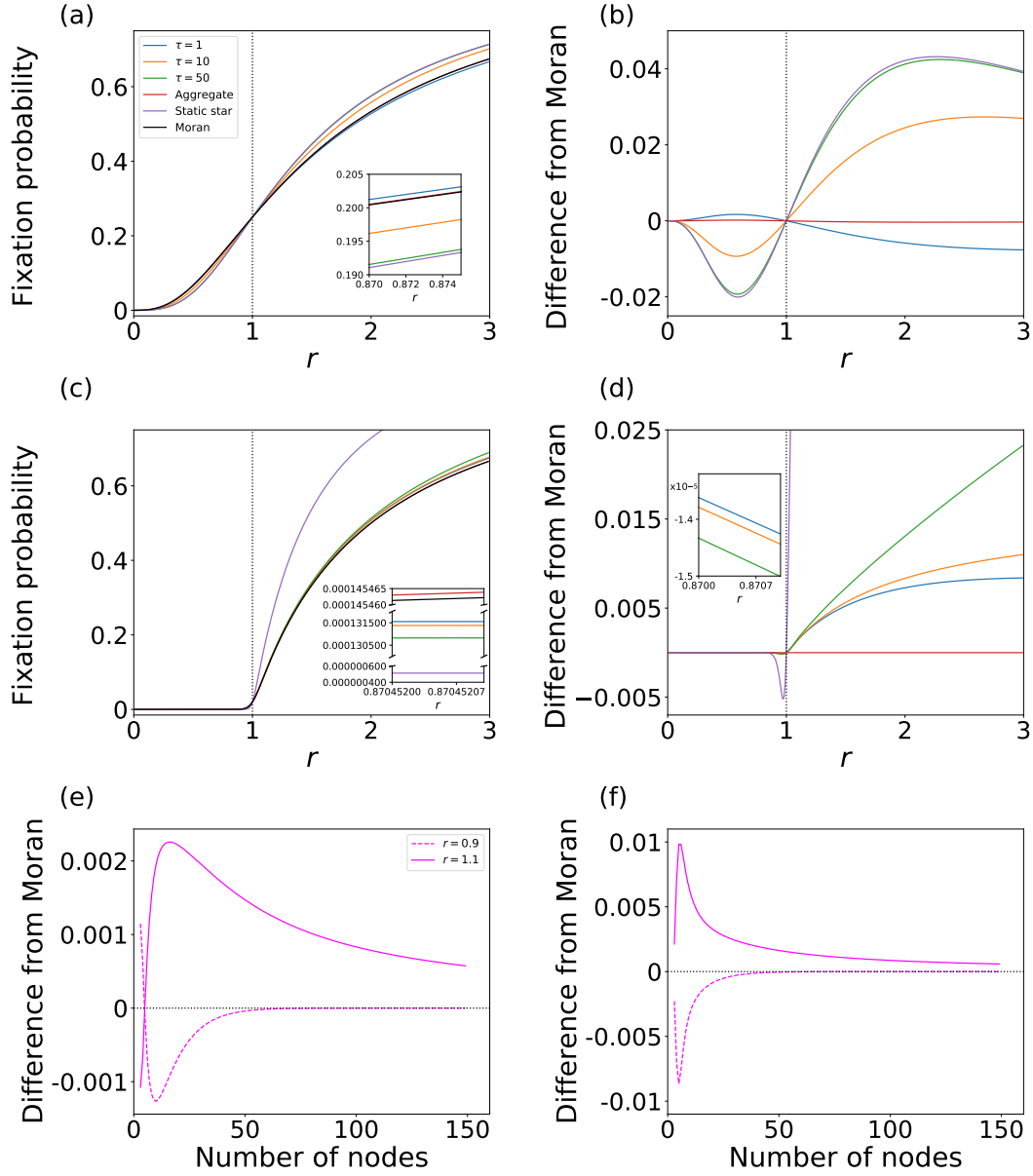


Figure 3: Fixation probability for switching networks in which G_1 is the star graph and G_2 is the complete graph. (a) Fixation probability for $N = 4$. (b) Difference in the fixation probability from the case of the Moran process for $N = 4$. (c) Fixation probability for $N = 50$. (d) Difference in fixation probability from the case of the Moran process for $N = 50$. In (a)–(d), we also show the results for G_1 (i.e., star graph) and the aggregate network, and the vertical lines at $r = 1$ are a guide to the eyes. The insets magnify selected ranges of $r < 1$. (e) and (f): Difference in the fixation probability for the switching network relative to the Moran process as a function of N at $r = 0.9$ and 1.1 . We set $\tau = 1$ in (e) and $\tau = 50$ in (f). In (e) and (f), the smallest value of N is three.

Eq. (12) represents the probability that the type of the hub changes from the resident to mutant. For this event to occur, one of the $j + k$ leaf nodes occupied by the mutant must be chosen as parent, which occurs with probability $r(j + k)/C_3$. Then, because any leaf node is only adjacent to the hub node, the hub node is always selected for death. Therefore, the probability of i changing from 0 to 1 is equal to $r(j + k)/C_3$. As another example, consider state $(1, j, k)$. For the state to change from $(1, j, k)$ to $(1, j + 1, k)$, the hub node, which the mutant type currently inhabits, must be selected as parent with probability r/C_4 . Then, one of the j leaf nodes of the resident type in V_1 must be selected for death, which occurs with probability $[(N_1 - 1) - j] / (N - 1)$. The fifth line of Eq. (12) is equal to the product of these two probabilities. One can similarly derive the other lines of Eq. (12).

The transition probability matrix for the complete bipartite graph is given by

$$T_{(i,j,k) \rightarrow (i',j',k')}^{(2)} = \begin{cases} \frac{rk}{C_3} \cdot \frac{1}{N_1} & \text{if } i = 0 \text{ and } i' = 1, \\ \frac{N_2 - k}{C_4} \cdot \frac{1}{N_1} & \text{if } i = 1 \text{ and } i' = 0, \\ \frac{N_2 - k}{C_3} \cdot \frac{j}{N_1} & \text{if } i = 0 \text{ and } j' = j - 1, \\ \frac{rk}{C_3} \cdot \frac{N_1 - 1 - j}{N_1} & \text{if } i = 0 \text{ and } j' = j + 1, \\ \frac{N_1 - j}{C_3} \cdot \frac{k}{N_2} & \text{if } i = 0 \text{ and } k' = k - 1, \\ \frac{rj}{C_3} \cdot \frac{N_2 - k}{N_2} & \text{if } i = 0 \text{ and } k' = k + 1, \\ \frac{N_2 - k}{C_4} \cdot \frac{j}{N_1} & \text{if } i = 1 \text{ and } j' = j - 1, \\ \frac{rk}{C_4} \cdot \frac{N_1 - 1 - j}{N_1} & \text{if } i = 1 \text{ and } j' = j + 1, \\ \frac{N_1 - 1 - j}{C_4} \cdot \frac{k}{N_2} & \text{if } i = 1 \text{ and } k' = k - 1, \\ \frac{r(j+1)}{C_4} \cdot \frac{N_2 - k}{N_2} & \text{if } i = 1 \text{ and } k' = k + 1, \\ 1 - \sum_{\substack{(i'',j'',k'') \neq \\ (i,j,k)}} T_{(i,j,k) \rightarrow (i'',j'',k'')}^{(2)} & \text{if } (i',j',k') = (i,j,k). \\ 0 & \text{otherwise.} \end{cases} \quad (13)$$

The first line of Eq. (13) represents the probability that the type of the hub changes from the resident to mutant. For this event to occur, one of the k mutant nodes in V_2 must be selected as parent with probability rk/C_3 . Then, the hub node must be selected for death with probability $1/N_1$ because each node in V_2 is only adjacent to all the N_1 nodes in V_1 . Therefore, the probability of i changing from 0 to 1 is equal to $(rk/C_3) \cdot (1/N_1)$. As another example, consider state $(1, j, k)$, in which there are $j + k + 1$ mutants in total. For the state to change from $(1, j, k)$ to $(1, j + 1, k)$, one of the k mutant nodes in V_2 must first be selected as parent with probability rk/C_4 . Then, one of the j leaf nodes in V_1 of the resident type must be selected for death, which occurs with probability $(N_1 - 1 - j)/N_1$. The eighth line of Eq. (13) is equal to the product of these two probabilities. One can similarly derive the other lines of Eq. (13).

In Figs. 4(a) and 4(b), we show the fixation probability and its difference from the case of the Moran process, respectively, for the switching network in which G_1 is the star on $N = 4$ nodes and G_2 is the complete bipartite graph K_{N_1, N_2} with $N_1 = N_2 = 2$. We set $\tau = 1, 10$, and 50 , and varied r . We also show the results for G_1 , G_2 , and the aggregate network in these figures for comparison. We find that $(G_1, G_2, 1)$ is a suppressor. In contrast, G_1 is an amplifier, and G_2 is neutral (i.e., equivalent to the Moran process). In fact, no static unweighted network with five nodes or less is a

suppressor [27]. Because the aggregate network is an amplifier, albeit a weak one, the suppressing effect of $(G_1, G_2, 1)$ owes to the time-varying nature of the switching network. Similar to the case in which G_2 is the complete graph shown in Fig. 3, $(G_1, G_2, 10)$ and $(G_1, G_2, 50)$ are amplifiers, and the behavior of $(G_1, G_2, 50)$ is close to that for G_1 , i.e., the star graph.

In Figs. 4(c) and 4(d), we show the fixation probability and its difference from the case of the Moran process, respectively, for $N_1 = N_2 = 20$. In contrast to the case of $N_1 = N_2 = 2$, the switching network with $N_1 = N_2 = 20$ is an amplifier for the three values of τ . Furthermore, in contrast to when $N_1 = N_2 = 2$, the fixation probabilities for the switching networks are closer to those for the Moran process than to those for the star graph.

These results for the switching networks with $N = 4$ and $N = 40$ nodes remain similar for switching networks (G_2, G_1, τ) , as we show in Figs. A1(c) and A1(d).

To examine the dependence of the fixation probability on the number of nodes, we show in Fig. 4(e) the difference between the fixation probability for the present switching network and that for the Moran process as we vary N . We set $\tau = 1$ and $N_1 = N_2 = N/2 \geq 2$, and compute the fixation probability at $r = 0.9$ and $r = 1.1$. Figure 4(e) indicates that the switching network is a suppressor only when $N_1 = N_2 = 2$ (i.e., $N = 4$) and amplifier for any larger N . When we allow $N_1 \neq N_2$, we found just one additional suppressor apart from $(N_1, N_2) = (2, 2)$ under the constraints $\tau = 1$ and $2 \leq N_1, N_2 \leq 10$, which is $(N_1, N_2) = (3, 2)$ (see Fig. A2(b)). With $\tau = 50$, this switching network is amplifier for any N (see Fig. 4(f)).

4.3 Empirical temporal networks

4.3.1 Construction of switching networks

Finally, we numerically simulate the birth-death process on four switching networks informed by empirical temporal network data. We split each of the temporal network data set into two static networks (V_1, E_1) and (V_2, E_2) , where (V_1, E_1) contains the first half of the time-stamped edges in terms of the time, (V_2, E_2) containing the second half of the time-stamped edges, V_1 and V_2 are sets of nodes, and E_1 and E_2 are sets of edges. For simplicity, we regard (V_1, E_1) and (V_2, E_2) as unweighted networks.

For two of the four empirical switching networks, both V_1 and V_2 contain all nodes. In this case, we switch between $G_1 \equiv (V_1, E_1)$ and $G_2 \equiv (V_2, E_2)$. For the other two empirical switching networks, either V_1 or V_2 misses some nodes in the original temporal network. In this case, we construct switching networks in the following two manners. With the first method, we only use the nodes in $V_1 \cap V_2$ and the edges that exist between pairs of nodes in $V_1 \cap V_2$ as G_1 and G_2 . For each of the two empirical data sets for which V_1 or V_2 misses some nodes, we have confirmed that the first and second halves of the static networks induced on $V_1 \cap V_2$ created with this method are connected networks. With the second method, we use all nodes for both G_1 and G_2 . In other words, we set $G_1 = (V_1 \cup V_2, E_1)$ and $G_2 = (V_1 \cup V_2, E_2)$. Therefore, if $v \in V_1$ and $v \notin V_2$, for example, then v is an isolated node in G_2 . Except with special initial conditions, the fixation of either type never occurs in a static network with isolated nodes. However, the fixation does occur in the switching network if the aggregate network is connected, which we have confirmed to be the case for all our empirical data sets.

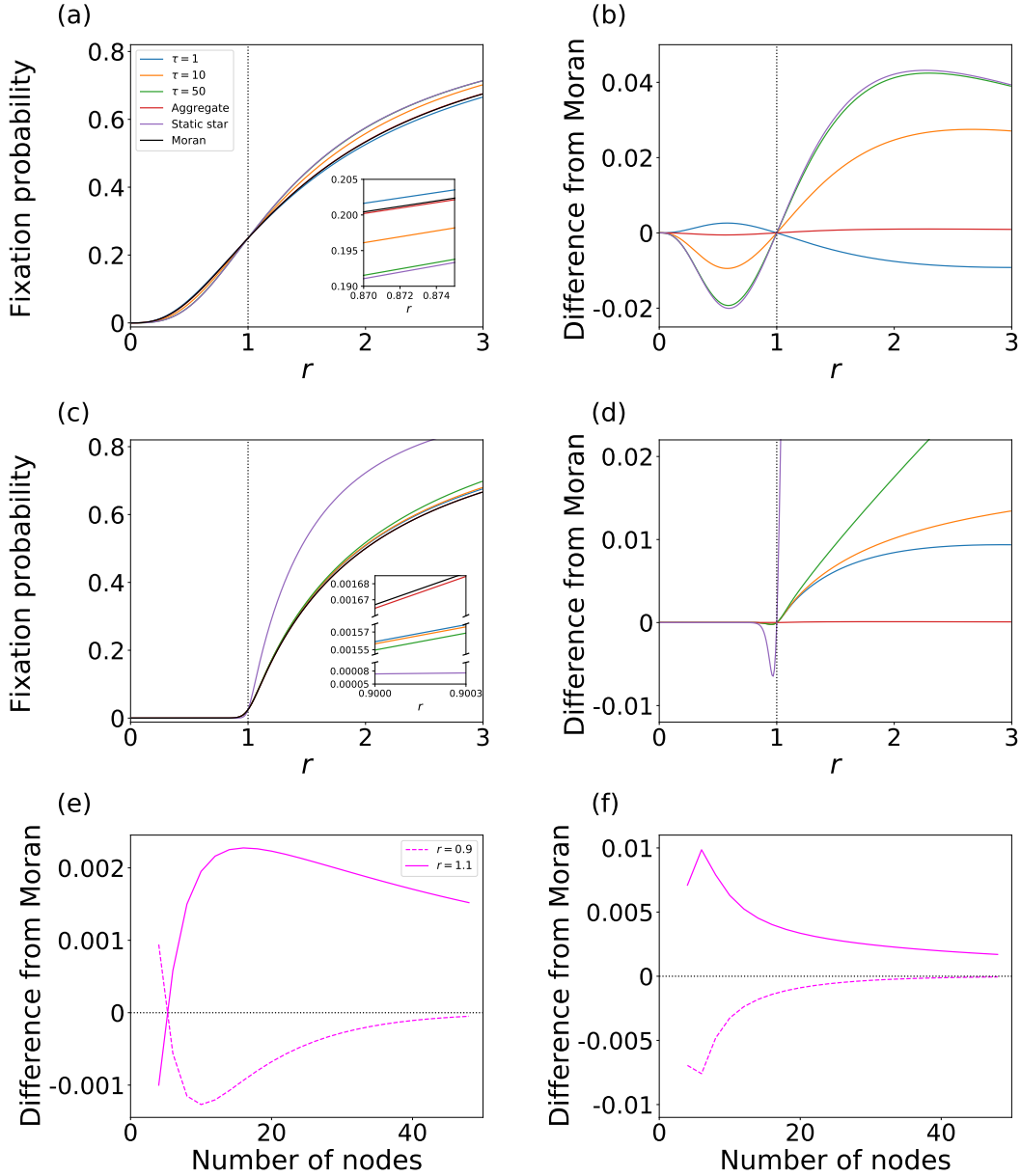


Figure 4: Fixation probability for switching networks in which G_1 is the star graph and G_2 is the complete bipartite graph. (a) Fixation probability for $N_1 = N_2 = 2$. (b) Difference in the fixation probability from the case of to the Moran process for $N_1 = N_2 = 2$. (c) Fixation probability for $N_1 = N_2 = 20$. (d) Difference in the fixation probability from the case of the Moran process for $N_1 = N_2 = 20$. (e) and (f): Difference in the fixation probability for the switching network relative to the Moran process as a function of N at $r = 0.9$ and 1.1 . We set $\tau = 1$ in (e) and $\tau = 50$ in (f). In (e) and (f), the smallest value of N is four.

4.3.2 Simulation procedure

As the initial condition, we place a mutant on one node selected uniformly at random and all the other $N - 1$ nodes are of the resident type. Then, we run the birth-death process until all nodes were of the same type. We carried out 2×10^5 such runs in parallel on 56 cores, giving us a total of 112×10^5 runs, for each network and each value of r . We numerically calculated the fixation probability as the fraction of runs in which the mutant fixates. We simulated the switching networks with $\tau \in \{1, 10, 50\}$ and $r \in \{0.7, 0.8, 0.9, 1, 1.1, 1.2, 1.3, 1.4, 1.5, 1.6, 1.7\}$ for all the networks except the hospital network of 75 nodes. For the hospital network, we omitted $r = 1.6$ and 1.7 due to high computational cost.

4.3.3 Data

The ants' colony data, which we abbreviate as ant [59], has 39 nodes and 330 time-stamped edges. Each node represents an ant in a colony. An edge represents a trophallaxis event, which was recorded when the two ants were engaged in mandible-to-mandible contact for greater than one second. The first and second halves of the data have 34 nodes each.

The second data is the contacts between members of five households in the Matsangoni sub-location within the Kilifi Health and Demographic Surveillance Site (KHDSS) in coastal Kenya [60]. A household was defined as the group of individuals who ate from the same kitchen [60]. Each participant in the study had a wearable sensor that detected the presence of another sensor within approximately 1.5 meters. Each node is an individual in a household. An edge represents a time-stamped contact between two individuals. There were 47 nodes. There were 219 time-stamped edges representing contacts between pairs of individuals in different households and 32,426 time-stamped edges between individuals of the same households. Both the first and second halves contain all the 47 nodes and are connected networks as static network owing to the relatively large number of time-stamped edges.

The third data is a mammalian temporal network based on interaction between raccoons [61]. A node represents a wild raccoon. The time-stamped events were recorded whenever two raccoons came within approximately 1 to 1.5 meters for more than one second, using proximity logging collars that were placed on raccoons. The recording was made in Ned Brown Forest Preserve in suburban Cook County, Illinois, USA, from July 2004 to July 2005. There are 24 nodes and 2,000 time-stamped edges. Both the first and second halves of the data contain all the 24 nodes and are connected networks as static network.

The fourth data is a contact network in a hospital [62]. The data were recorded in a geriatric unit of a university hospital in Lyon, France, from December 6, 2010 at 1 pm to December 10, 2010 at 2 pm. The unit contained 19 out of the 1,000 beds in the hospital. During the recording period, 50 professionals worked in the unit, and 31 patients were admitted. Forty-six among the 50 professionals and 29 among the 31 patients participated in the study. Therefore, the network had 75 nodes in total. The professionals comprised of 27 nurses or nurses' aides, 11 medical doctors, and 8 administrative staff members. An edge represents a time-stamped contact between two individuals; there are 32,424 time-stamped edges. The first and second halves of the data contain 50 nodes each.

We obtained the ant, raccoon, and hospital data from <https://networkrepository.com/> [63]. We obtained the Kilifi data from <https://www.sociopatterns.org/>.

4.3.4 Numerical results

We investigate the fixation probability on the switching networks with $\tau = 1, 10,$ and 50 , static networks G_1 and G_2 , and the aggregate network. We remind that the aggregate network is a static weighted network, whereas G_1 and G_2 are unweighted networks. For the ant and hospital data, the switching networks constructed with the second method are different from those constructed with the first method. For these two data sets, fixation does not occur on G_1 and G_2 because they miss some nodes. Therefore, we do not analyze the fixation probability on G_1 and G_2 for these data sets.

We show in Figs. 5(a) and 5(b) the fixation probability on the ant switching networks constructed with the first and second methods, respectively. Because we are interested in whether the switching networks are amplifiers or suppressors, we only show the difference between the fixation probability on the given network and that for the Moran process in Fig. 5. Figure 5(a) indicates that the switching networks are amplifiers but less amplifying than each of its constituent static networks, G_1 and G_2 . Another observation is that the fixation probability on the static aggregate network is close to that on the switching networks. In this sense, the switching networks do not yield surprising results. The switching networks are more strongly amplifying when τ is larger. Moreover, the fixation probability on the switching network is closer to that on G_1 when τ is larger. This result is expected because the evolutionary dynamics is the same between the switching networks and G_1 in the first τ time steps. For the switching networks constructed with the second method, Fig. 5(b) shows that the switching networks are amplifiers and more amplifying than the static aggregate network. This result is qualitatively different from that for the switching networks constructed with the first method shown in Fig. 5(a).

We show the results for the Kilifi networks in Fig. 5(c). Because the first and second methods yield the same G_1 and G_2 for the Kilifi data, we only present the results for the first method for this data set and also for the next one (i.e., racoon networks). The figure indicates that the switching networks are amplifiers but less amplifying than G_1 and G_2 and similarly amplifying compared to the aggregate network. These results are similar to those for the ant networks shown in Fig. 5(a).

We show the results for the racoon networks in Fig. 5(d). We find that the switching networks are amplifiers but less amplifying than G_1 and G_2 , similar to the case of the ant and Kilifi networks. We also find that the switching networks are more amplifying than the aggregate network.

We show the results for the hospital switching networks in Figs. 5(e) and 5(f). The results for the switching networks constructed with the first method (see Fig. 5(e)) are similar to those for the racoon networks shown in Fig. 5(d). The switching networks constructed with the second method (see Fig. 5(f)) are more amplifying than the aggregate network, similar to the case of the ant networks generated by the same method (see Fig. 5(b)).

In sum, for these empirical temporal networks, we did not find a surprising result that the fixation probability for the switching networks is not an interpolation of those for the two static networks G_1 and G_2 . However, the fixation probability for the empirical switching networks depends on the τ value and deviates from the prediction from the aggregate network in multiple ways.

5 Discussion

We have shown that, under the birth-death updating rule and uniform initialization, a majority of the switching networks on six nodes are suppressors of natural selection. This result contrasts with the case of static networks, for which there exists only one suppressor on six nodes [27]. We

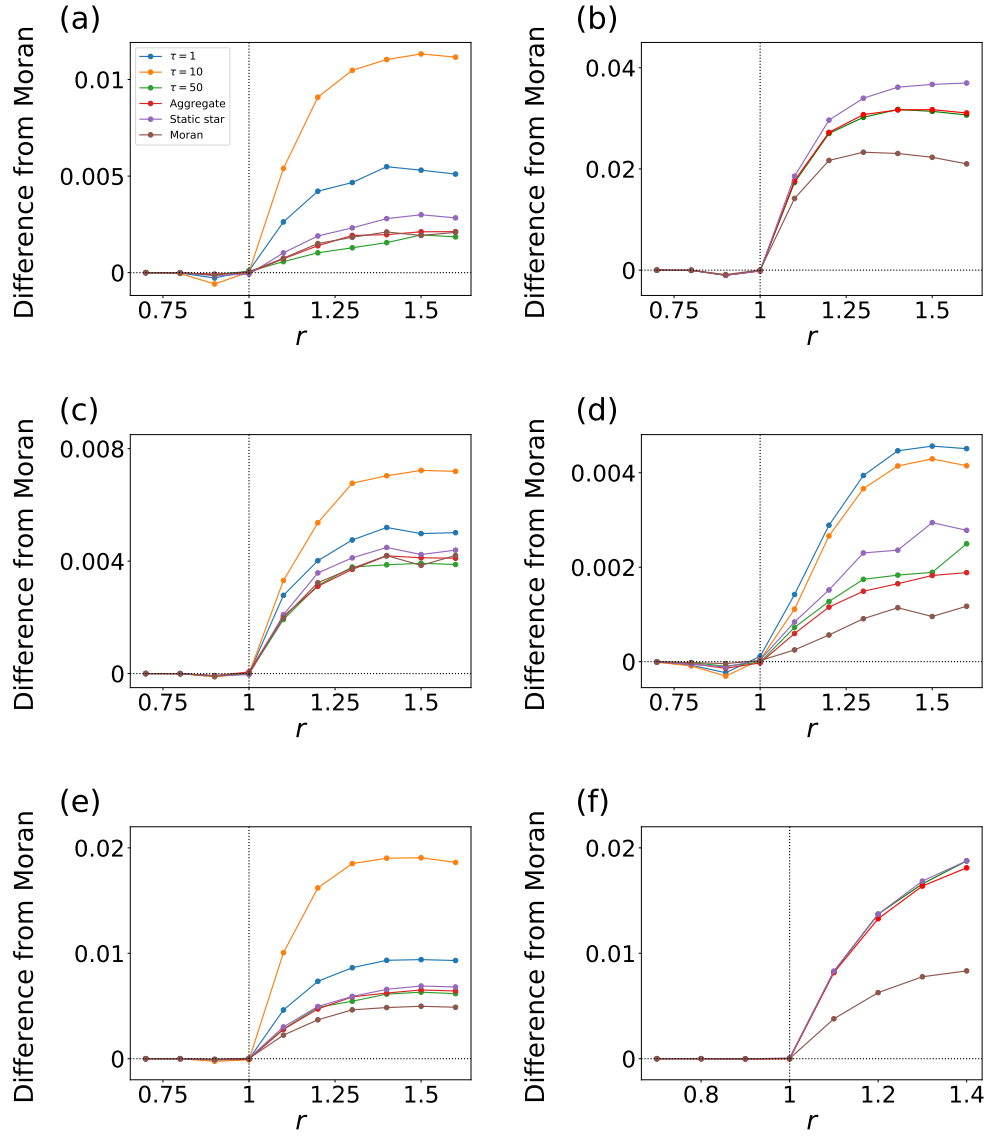


Figure 5: Fixation probability on empirical switching networks. In each panel, we show the difference in the fixation probability from the case of the Moran process as a function of r . (a) Ant networks constructed with the first method. (b) Ant networks constructed with the second method. (c) Kilifi switching networks. (d) Raccoon networks. (e) Hospital networks constructed with the first method. (f) Hospital networks constructed with the second method. We compared the fixation probability on switching networks with $\tau \in \{1, 10, 50\}$, G_1 , G_2 , and the aggregate network in each panel.

also found that switching networks alternating between the star graph and the complete graph and those alternating between the star graph and the complete bipartite graph are suppressors when the number of nodes, N , is small. When N is larger, the same switching networks are amplifiers but less amplifying than the star graph. Among the empirical networks that we analyzed, we did not find any suppressors. However, these switching networks were notably less amplifying than the constituent static networks G_1 and G_2 . In fact, the less amplifying nature of switching networks is largely explained by the aggregate weighted network, or the static network obtained by the superposition of G_1 and G_2 . Therefore, our results for the empirical switching networks are not surprising. The result that the switching network composed of two amplifying static networks can be suppressor is our main finding. Because all the instances that we have found are small networks, searching suppressing switching networks with larger N including systematically constructing such instances remains future work.

We considered exogenous changes of the network over time in this study. Another opportunity of research is to assume that the change of the network structure over time is driven by the state of the system, which is referred to as adaptive networks [64,65]. The recent modeling framework inspired by biological examples in which the residents and mutants use different static networks defined on the same node set [66,67] can be interpreted as an example of fixation dynamics on adaptive networks. Allowing nodes to stochastically sever and create edges they own as the node’s type flips from the resident to mutant and vice versa may lead to new phenomena in fixation dynamics. Such models have been extensively studied for evolutionary games on dynamic networks [17–23].

We recently found that most hypergraphs are suppressors under the combination of a birth-death process and uniform initialization, which are the conditions under which most of conventional networks are amplifiers [54]. It has been longer known that most undirected networks are suppressors under the death-birth process [25] and in directed networks under various imitation rules including birth-death processes [68]. The degree of amplification and suppression also depends on the initialization [24,31]. For example, non-uniform initializations can make the star, which is a strong amplifier under the birth-death process and uniform initialization, a suppressor [24]. Furthermore, it has been shown that the amplifiers are transient and bounded [69]. Our results suggest that small temporal networks are another major case in which suppressors are common. These results altogether encourage us to explore different variants of network models and evolutionary processes to clarify how common amplifiers are. This task warrants future research.

Funding

N.M. acknowledges support from AFOSR European Office (under Grant No. FA9550-19-1-7024), the Japan Science and Technology Agency (JST) Moonshot R&D (under Grant No. JPMJMS2021), and the National Science Foundation (under Grant No. 2052720 and 2204936).

Appendices

A1. Switching networks in which the first network is the star graph

In this section, we consider switching networks (G_1, G_2, τ) in which G_1 is the complete graph and G_2 is the star graph. We show the difference in the fixation probability from the case of the Moran process for the switching networks with $N = 4$ and $N = 50$ in Figs. A1(a) and A1(b), respectively.

With $N = 4$, we find that $(G_1, G_2, 10)$ and $(G_1, G_2, 50)$ are amplifiers and that $(G_1, G_2, 1)$ is a suppressor (see Fig. A1(a)). The aggregate network is a weak suppressor. With $N = 50$, we find that (G_1, G_2, τ) for all the three τ values (i.e., $\tau \in \{1, 10, 50\}$) are amplifiers and that the aggregate network is a weak suppressor (see Fig. A1(b)). These results are qualitatively the same as those for the switching networks in which the order of G_1 and G_2 is the opposite, shown in Fig. 3. A main difference is that, when $\tau = 50$, the fixation probability is reasonably close to that for the Moran process in the case of the present switching network because G_1 is a regular graph and therefore equivalent to the Moran process. In contrast, in Fig. 3, the switching network is much more amplifying because G_1 is the star graph, which is a strong amplifier.

We show in Figs. A1(c) and A1(d) the results for the switching networks with $N = 4$ and $N = 40$, respectively, in which G_1 is the complete bipartite graph and G_2 is the star graph. With $N = 4$, we find that $(G_1, G_2, 1)$ is a suppressor, $(G_1, G_2, 10)$ and $(G_1, G_2, 50)$ are amplifiers $\tau = 50$, and the aggregate network is a weak amplifier (see Fig. A1(c)). With $N = 40$, we find that (G_1, G_2, τ) with $\tau \in \{1, 10, 50\}$ is an amplifier and that the aggregate network is a weak amplifier (see Fig. A1(d)). These results are similar to those for the switching networks in which the order of G_1 and G_2 is the opposite, shown in Figs. 4(a) and 4(b). Similar to Figs. A1(a) and A1(b), with $\tau = 50$, the present switching networks are close in behavior to the Moran process because G_1 is a regular network. This result contrasts to the corresponding result for the order-swapped switching network with $\tau = 50$, which is a relatively strong amplifier because G_1 is the star graph (see Figs. 4(a) and 4(b)).

A2. Further examples of small amplifying switching networks in which G_1 is the star graph

In Fig. A2(a), we show the difference in the fixation probability from the case of the Moran process for the switching networks in which G_1 is the star graph and G_2 is the complete graph on $N = 3$ nodes. We also plot the results for G_1 , G_2 , and the aggregate network. It is known that G_1 is an amplifier [1] and that G_2 is equivalent to the Moran process. In contrast, the switching network with $\tau = 1$ and the aggregate network are suppressors. The aggregate network is much less suppressing than the switching network. The switching networks with $\tau \in \{10, 50\}$ are amplifiers.

In Fig. A2(b), we show the results for the switching networks in which G_1 is the star graph and G_2 is the complete bipartite graph, $K_{(3,2)}$, on $N = 5$ nodes. Note that both G_1 (i.e., star) [1] and G_2 (i.e., complete bipartite graph $K_{(3,2)}$) [70] are amplifiers. In contrast, as in Fig. A2(a), the switching network with $\tau = 1$ (but not with $\tau \in \{10, 50\}$) and the aggregate network are suppressors, and the aggregate network is only weakly suppressing.

References

- [1] E. Lieberman, C. Hauert, and M. A. Nowak. Evolutionary dynamics on graphs. *Nature*, 433(7023):312–316, 2005.
- [2] M. Nowak. *Evolutionary Dynamics: Exploring the Equations of Life*. Harvard University Press, Cambridge, MA, 2006.
- [3] M. A. Nowak, C. E. Tarnita, and T. Antal. Evolutionary dynamics in structured populations. *Philosophical Transactions of the Royal Society B*, 365(1537):19–30, 2010.

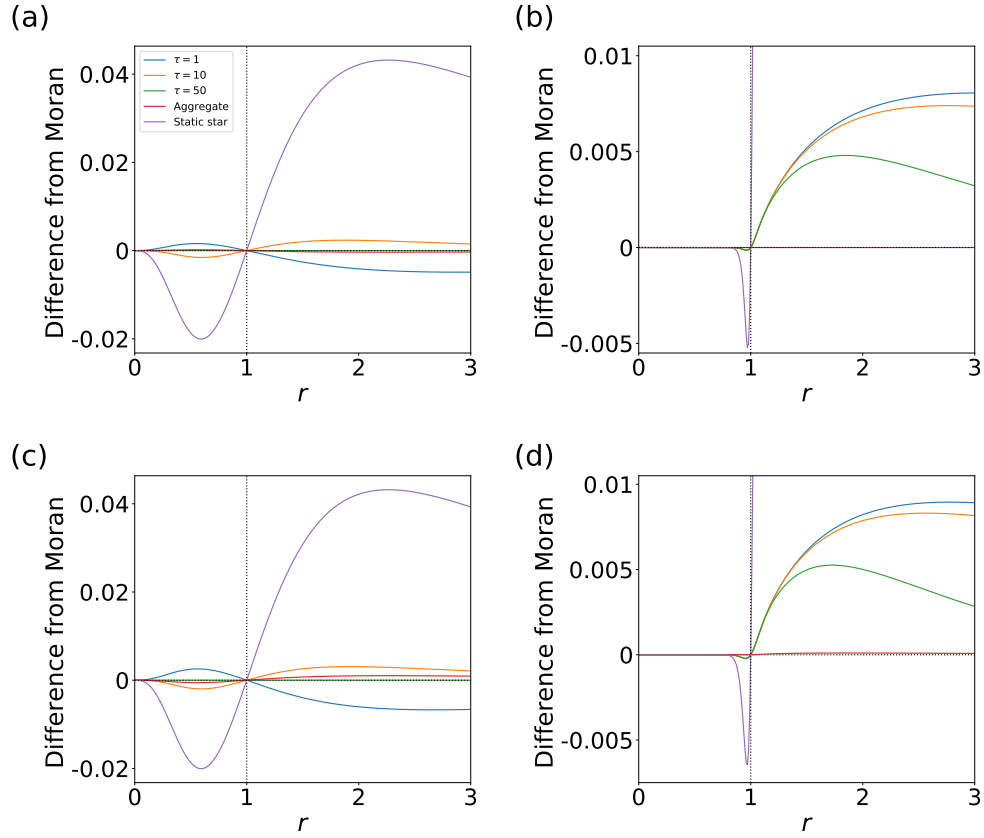


Figure A1: Fixation probability for switching networks in which G_2 is the star graph. In each panel, we show the difference in the fixation probability from the case of the Moran process. (a) $N = 4$ and the complete graph as G_1 . (b) $N = 50$ and the complete graph as G_1 . (c) $N_1 = N_2 = 2$ and the complete bipartite graph as G_1 . (d) $N_1 = N_2 = 20$ and the complete bipartite graph as G_1 . We do not show the result for G_1 because both the complete graph and the complete bipartite graph are equivalent to the Moran process such that the difference from the Moran process is 0 for any r .

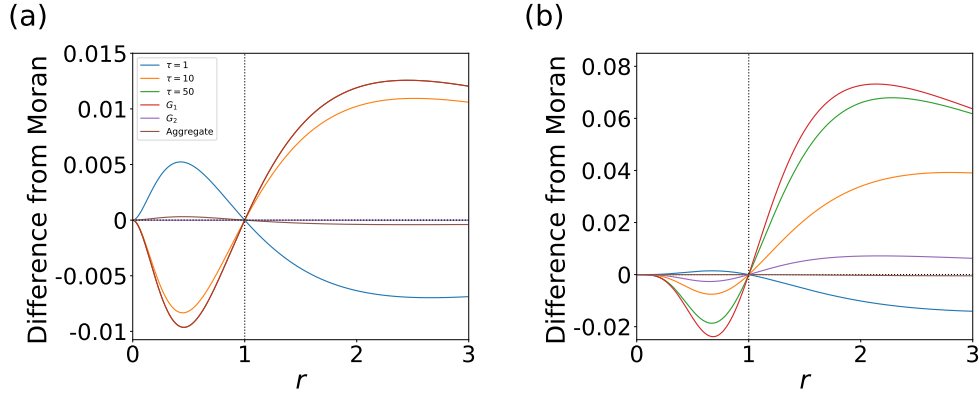


Figure A2: Fixation probability as a function of r for two small switching networks. (a) Switching network with $N = 3$ in which G_1 is the star graph and G_2 is the complete graph. (b) Switching network with $N = 5$ in which G_1 is the star graph and G_2 is the complete bipartite graph $K_{(3,2)}$.

- [4] P. Shakarian, P. Roos, and A. Johnson. A review of evolutionary graph theory with applications to game theory. *Biosystems*, 107(2):66–80, 2012.
- [5] M. Perc, J. Gómez-Gardenes, A. Szolnoki, L. M. Floría, and Y. Moreno. Evolutionary dynamics of group interactions on structured populations: a review. *Journal of the Royal Society Interface*, 10(80):20120997, 2013.
- [6] R. Durrett. Stochastic spatial models. *SIAM Review*, 41(4):677–718, 1999.
- [7] T. Antal, S. Redner, and V. Sood. Evolutionary dynamics on degree-heterogeneous graphs. *Physical Review Letters*, 96(18):188104, 2006.
- [8] V. Sood, T. Antal, and S. Redner. Voter models on heterogeneous networks. *Physical Review E*, 77(4):041121, 2008.
- [9] C. Castellano, S. Fortunato, and V. Loreto. Statistical physics of social dynamics. *Reviews of Modern Physics*, 81(2):591–646, 2009.
- [10] P. Holme and J. Saramäki. Temporal networks. *Physics Reports*, 519(3):97–125, 2012.
- [11] P. Holme and J. Saramäki. *Temporal Networks*. Springer-Verlag, Berlin, Germany, 2013.
- [12] P. Holme. Modern temporal network theory: a colloquium. *European Physical Journal B*, 88:234, 2015.
- [13] N. Masuda and P. Holme. *Introduction to Temporal Network Epidemiology*. Springer, Singapore, 2017.
- [14] M. Karsai, H. H. Jo, and K. Kaski. *Bursty Human Dynamics*. Springer International Publishing, Cham, Switzerland, 2018.

- [15] P. Holme and J. Saramäki. *Temporal Network Theory*. Springer, New York, NY, 2019.
- [16] R. Lambiotte and N. Masuda. *A Guide to Temporal Networks*. World Scientific, Singapore, 2021.
- [17] A. Cardillo, G. Petri, V. Nicosia, R. Sinatra, J. Gómez-Gardenes, and V. Latora. Evolutionary dynamics of time-resolved social interactions. *Physical Review E*, 90(5):052825, 2014.
- [18] A. Li, L. Zhou, Q. Su, S. P. Cornelius, Y. Y. Liu, L. Wang, and S. A. Levin. Evolution of cooperation on temporal networks. *Nature Communications*, 11(1):2259, 2020.
- [19] T. Johnson and O. Smirnov. Temporal assortment of cooperators in the spatial prisoner’s dilemma. *Communications Biology*, 4(1):1283, 2021.
- [20] A. Sheng, A. Li, and L. Wang. Evolutionary dynamics on sequential temporal networks. *arXiv preprint arXiv:2110.05995*, 2021.
- [21] F. C. Santos, J. M. Pacheco, and T. Lenaerts. Cooperation prevails when individuals adjust their social ties. *PLoS Computational Biology*, 2(10):e140, 2006.
- [22] J. M. Pacheco, A. Traulsen, and M. A. Nowak. Coevolution of strategy and structure in complex networks with dynamical linking. *Physical Review Letters*, 97(25):258103, 2006.
- [23] F. Fu, T. Wu, and L. Wang. Partner switching stabilizes cooperation in coevolutionary prisoner’s dilemma. *Physical Review E*, 79(3):036101, 2009.
- [24] B. Adlam, K. Chatterjee, and M. A. Nowak. Amplifiers of selection. *Proceedings of the Royal Society A*, 471(2181):20150114, 2015.
- [25] L. Hindersin and A. Traulsen. Most undirected random graphs are amplifiers of selection for birth-death dynamics, but suppressors of selection for death-birth dynamics. *PLoS Computational Biology*, 11(11):e1004437, 2015.
- [26] B. Allen, C. Sample, P. Steinhagen, J. Shapiro, M. King, T. Hedspeth, and M. Goncalves. Fixation probabilities in graph-structured populations under weak selection. *PLoS Computational Biology*, 17(2):e1008695, 2021.
- [27] F. A. Cuesta, P. G. Sequeiros, and Á. L. Rojo. Suppressors of selection. *PLoS ONE*, 12(7):e0180549, 2017.
- [28] G. Giakkoupis. Amplifiers and suppressors of selection for the moran process on undirected graphs. *arXiv preprint arXiv:1611.01585*, 2016.
- [29] A. Galanis, A. Göbel, L. A. Goldberg, J. Lapinskas, and D. Richerby. Amplifiers for the moran process. *Journal of the ACM*, 64(1):5, 2017.
- [30] A. Pavlogiannis, J. Tkadlec, K. Chatterjee, and M. A. Nowak. Amplification on undirected population structures: comets beat stars. *Scientific Reports*, 7(1):82, 2017.
- [31] A. Pavlogiannis, J. Tkadlec, K. Chatterjee, and M. A. Nowak. Construction of arbitrarily strong amplifiers of natural selection using evolutionary graph theory. *Communications Biology*, 1(1):71, 2018.

- [32] L. A. Goldberg, J. Lapinskas, J. Lengler, F. Meier, K. Panagiotou, and P. Pfister. Asymptotically optimal amplifiers for the moran process. *Theoretical Computer Science*, 758:73–93, 2019.
- [33] F. A. Cuesta, P. G. Sequeiros, and Á. L. Rojo. Evolutionary regime transitions in structured populations. *PLoS ONE*, 13(11):e0200670, 2018.
- [34] H. Ohtsuki, C. Hauert, E. Lieberman, and M. A. Nowak. A simple rule for the evolution of cooperation on graphs and social networks. *Nature*, 441(7092):502–505, 2006.
- [35] R. Olfati-Saber. Evolutionary dynamics of behavior in social networks. In *Proceedings of the 46th IEEE Conference on Decision and Control*, pages 4051–4056. IEEE, 2007.
- [36] M. Porfiri, D. J. Stilwell, E. M. Bollt, and J. D. Skufca. Random talk: Random walk and synchronizability in a moving neighborhood network. *Physica D*, 224(1-2):102–113, 2006.
- [37] D. J. Stilwell, E. M. Bollt, and D. G. Roberson. Sufficient conditions for fast switching synchronization in time-varying network topologies. *SIAM Journal on Applied Dynamical Systems*, 5(1):140–156, 2006.
- [38] N. Masuda, K. Klemm, and V. M. Eguíluz. Temporal networks: Slowing down diffusion by long lasting interactions. *Physical Review Letters*, 111:188701, 2013.
- [39] M. Hasler, V. Belykh, and I. Belykh. Dynamics of stochastically blinking systems. part I: Finite time properties. *SIAM Journal on Applied Dynamical Systems*, 12(2):1007–1030, 2013.
- [40] M. Hasler, V. Belykh, and I. Belykh. Dynamics of stochastically blinking systems. part II: Asymptotic properties. *SIAM Journal on Applied Dynamical Systems*, 12(2):1031–1084, 2013.
- [41] N. Masuda. Accelerating coordination in temporal networks by engineering the link order. *Scientific Reports*, 6(1):22105, 2016.
- [42] N. Perra, A. Baronchelli, D. Mocanu, B. Gonçalves, R. Pastor-Satorras, and A. Vespignani. Random walks and search in time-varying networks. *Physical Review Letters*, 109(23):238701, 2012.
- [43] L. E. C. Rocha and N. Masuda. Random walk centrality for temporal networks. *New Journal of Physics*, 16(6):063023, 2014.
- [44] L. Alessandretti, K. Sun, A. Baronchelli, and N. Perra. Random walks on activity-driven networks with attractiveness. *Physical Review E*, 95(5):052318, 2017.
- [45] L. Speidel, K. Klemm, V. M. Eguíluz, and N. Masuda. Temporal interactions facilitate endemicity in the susceptible-infected-susceptible epidemic model. *New Journal of Physics*, 18(7):073013, 2016.
- [46] T. Onaga, J. P. Gleeson, and N. Masuda. Concurrency-induced transitions in epidemic dynamics on temporal networks. *Physical Review Letters*, 119(10):108301, 2017.
- [47] E. Valdano, L. Ferreri, C. Poletto, and V. Colizza. Analytical computation of the epidemic threshold on temporal networks. *Physical Review X*, 5(2):021005, 2015.

- [48] V. L. J. Somers and I. R. Manchester. Sparse resource allocation for spreading processes on temporal-switching networks. *arXiv preprint arXiv:2302.02079*, 2023.
- [49] A. Li, S. P. Cornelius, Y. Y. Liu, L. Wang, and A. L. Barabási. The fundamental advantages of temporal networks. *Science*, 358(6366):1042–1046, 2017.
- [50] J. Petit, B. Lauwens, D. Fanelli, and T. Carletti. Theory of turing patterns on time varying networks. *Physical Review Letters*, 119(14):148301, 2017.
- [51] L. Hindersin, M. Möller, A. Traulsen, and B. Bauer. Exact numerical calculation of fixation probability and time on graphs. *Biosystems*, 150:87–91, 2016.
- [52] M. Broom and J. Rychtář. An analysis of the fixation probability of a mutant on special classes of non-directed graphs. *Proceedings of the Royal Society A*, 464(2098):2609–2627, 2008.
- [53] H. M. Taylor and S. Karlin. *An Introduction to Stochastic Modeling*. Academic Press Inc., San Diego, CA, third edition, 1998.
- [54] R. Liu and N. Masuda. Fixation dynamics on hypergraphs. *arXiv preprint arXiv:2301.05343*, 2023.
- [55] B. Voorhees. Birth–death fixation probabilities for structured populations. *Proceedings of the Royal Society A*, 469(2153):20120248, 2013.
- [56] M. Broom and J. Rychtář. *Game-Theoretical Models in Biology*. Chapman and Hall/CRC, Boca Raton, FL, second edition, 2022.
- [57] B. Allen, G. Lippner, and M. A. Nowak. Evolutionary games on isothermal graphs. *Nature Communications*, 10(1):5107, 2019.
- [58] F. A. Cuesta, P. G. Sequeiros, and Á. L. Rojo. An accurate database of the fixation probabilities for all undirected graphs of order 10 or less. In I. Rojas and F. Ortuño, editors, *Bioinformatics and Biomedical Engineering*, pages 209–220, Cham, Switzerland, 2017. Springer International Publishing.
- [59] L. E. Quevillon, E. M. Hanks, S. Bansal, and D. P. Hughes. Social, spatial and temporal organization in a complex insect society. *Scientific Reports*, 5(1):13393, 2015.
- [60] M. C. Kiti, M. Tizzoni, T. M. Kinyanjui, D. C. Koech, P. K. Munywoki, M. Meriac, L. Cappa, A. Panisson, A. Barrat, C. Cattuto, and D. J. Nokes. Quantifying social contacts in a household setting of rural kenya using wearable proximity sensors. *EPJ Data Science*, 5(1):21, 2016.
- [61] J. J. H. Reynolds, B. T. Hirsch, S. D. Gehrt, and M. E. Craft. Raccoon contact networks predict seasonal susceptibility to rabies outbreaks and limitations of vaccination. *Journal of Animal Ecology*, 84(6):1720–1731, 2015.
- [62] P. Vanhems, A. Barrat, C. Cattuto, J. F. Pinton, N. Khanafer, C. Régis, B. Kim, B. Comte, and N. Voirin. Estimating potential infection transmission routes in hospital wards using wearable proximity sensors. *PLoS ONE*, 8(9):e73970, 2013.

- [63] R. Rossi and N. Ahmed. The network data repository with interactive graph analytics and visualization. In *Proceedings of the AAAI Conference on Artificial Intelligence*, volume 29, page 4292–4293, 2015.
- [64] T. Gross and B. Blasius. Adaptive coevolutionary networks: a review. *Journal of the Royal Society Interface*, 5(20):259–271, 2008.
- [65] H. Sayama, I. Pestov, J. Schmidt, B. J. Bush, C. Wong, J. Yamanoi, and T. Gross. Modeling complex systems with adaptive networks. *Computers & Mathematics with Applications*, 65(10):1645–1664, 2013.
- [66] T. Melissourgos, S. E. Nikolettseas, C. L. Raptopoulos, and P. G. Spirakis. An extension of the moran process using type-specific connection graphs. *Journal of Computer and System Sciences*, 124:77–96, 2022.
- [67] J. Tkadlec, K. Kaveh, K. Chatterjee, and M. A. Nowak. Natural selection of mutants that modify population structure. *arXiv preprint arXiv:2111.10890*, 2021.
- [68] N. Masuda. Directionality of contact networks suppresses selection pressure in evolutionary dynamics. *Journal of Theoretical Biology*, 258(2):323–334, 2009.
- [69] J. Tkadlec, A. Pavlogiannis, K. Chatterjee, and M. A. Nowak. Limits on amplifiers of natural selection under death-birth updating. *PLoS Computational Biology*, 16(1):e1007494, 2020.
- [70] T. Monk, P. Green, and M. Paulin. Martingales and fixation probabilities of evolutionary graphs. *Proceedings of the Royal Society A*, 470(2165):20130730, 2014.